

Electron muon elastic scattering in one-loop QED with soft-photon corrections

LE Duc Truyen

Ho Chi Minh city University of Science
Department of Theoretical Physics


ICISE, Quy Nhon, Vietnam
Institute For Interdisciplinary Research in Science and Education

August 27, 2020

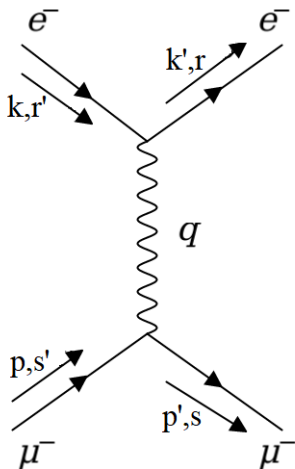


- 1 Leading order
- 2 Next-to-leading order
 - UV cancellation
 - IR cancellation
 - Numerical results
- 3 Conclusion and outlook

- At the next-to-leading order (NLO) level, we will meet UV and IR divergences and have to use some techniques to handle it.
- Recently, the new experiment MUonE has been proposed [1]¹ to measure precisely the running of the fine-structure constant at space-like momenta via the electron-muon elastic scattering.

¹[1] **G. Abbiendi et al.** "Measuring the leading hadronic contribution to the muon $g-2$ via μe scattering". *Eur. Phys. J. C*, 77(3):139, 2017. 

Leading order Feynman diagram



The averaged squared matrix :

$$|\bar{\mathcal{M}}|_{LO}^2 = \frac{8e^4}{t^2} \left[\frac{s^2}{4} + \frac{u^2}{4} + (m_\mu^2 + m_e^2)t - \frac{(m_\mu^2 + m_e^2)^2}{2} \right],$$

$$q^2 = t = -2|\vec{p}|^2 (1 - \cos \theta).$$

Cross section distributions

At leading order $e^- \mu^- \rightarrow e^- \mu^-$ scattering, we obtain the differential cross sections :

$$\frac{d\sigma}{d\cos\theta} = 4\pi \frac{\alpha^2}{t^2 s} \left[\frac{s^2}{4} + \frac{u^2}{4} + (m_\mu^2 + m_e^2)t - \frac{(m_\mu^2 + m_e^2)^2}{2} \right], \quad (1)$$

or :

$$\frac{d\sigma}{dt} = 4\pi \frac{1}{2|\vec{p}|^2} \frac{\alpha^2}{t^2 s} \left[\frac{s^2}{4} + \frac{u^2}{4} + (m_\mu^2 + m_e^2)t - \frac{(m_\mu^2 + m_e^2)^2}{2} \right], \quad (2)$$

with Mandelstam s, t, u and \vec{p} in Center of Mass frame (CMF).


Input parameters

For the MuonE experiment, we have the scattering of high-energy muons on electrons at rest. The energy of the incoming muon, we require $E_{\mu}^{\text{Beam}} = E_{\mu} = 150 \text{ GeV}$. For the numerical calculation, the input parameters are set to, the same as in [2]² :

$$\alpha \equiv \alpha(0) = 1/137.03599907430637, \quad m_e = 0.510998928 \text{ MeV}, \quad m_{\mu} = 105.6583715 \text{ MeV}. \quad (3)$$

The \sqrt{s} value is the colliding energy in the CMF of the MUonE experiment :

$$\sqrt{s} = \sqrt{m_e^2 + E_{\mu}^2 + 2m_e E_{\mu}} = 0.405541158 \text{ GeV}. \quad (4)$$

²[2] **Massimo Alacevich, et al.** *JHEP*, 02:155, 2019. 

LO numerical results

We provide a table of the differential cross section at different values of $\cos \theta$ in Tabs. (1) :

$\mu^- e^- \rightarrow \mu^- e^-$		
$\cos \theta$	$\frac{d\sigma}{d\cos\theta}(\cos\theta) \quad [\mu b]$	
	$m_e \neq 0$	$m_e = 0$
-1	0.3960810768531	0.3960806244802
-0.5	0.8012992639148	0.8012968782068
0	2.2195626924442	2.2195537662498
0.5	11.336969413281	11.336919475097
0.9602	2256.8970604919	2256.8871114676

Table 1: Differential cross section at different values of $\cos \theta$ (in the CMF)

For $m_e = 0$ case, we get rid of all m_e in Eqs. (1-2)

LO numerical cross section comparison

In Lab frame (where the initial electron is at rest), we request :
 $\theta_e, \theta_\mu < 100$ mrad and $E_e > 0.2$ GeV (corresponding to $\cos \theta \lesssim 0.997$ in CMF) for the final particles [2].

$\mu^- e^- \rightarrow \mu^- e^-$		
Cross section	Analytical result using Mathematica	Monte-Carlo simulation [2]
$\sigma_{LO}^{QED}(m_e \neq 0)$	1265.0603541	1265.060312(7)
$\sigma_{LO}^{QED}(m_e = 0)$	1264.9381128	(-)

Table 2: Leading order cross section for MuonE experiment.

Using the above MuonE experiment setup, we can now compare our analytical result with the numerical simulation of [2].

LO numerical cross section comparison

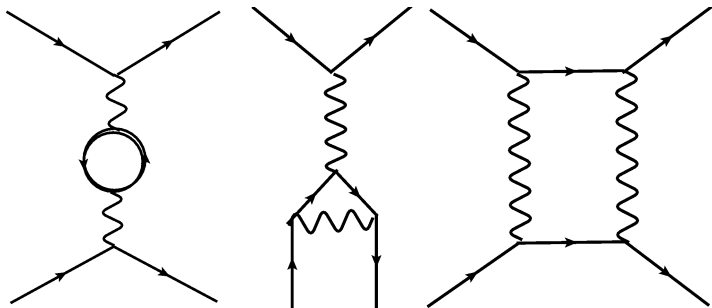
In Lab frame (where the initial electron is at rest), we request :
 $\theta_e, \theta_\mu < 100$ mrad and $E_e > 0.2$ GeV (corresponding to $\cos \theta \lesssim 0.997$ in CMF) for the final particles [2].

$\mu^- e^- \rightarrow \mu^- e^-$		
Cross section	Analytical result using Mathematica	Monte-Carlo simulation [2]
$\sigma_{LO}^{QED}(m_e \neq 0)$	1265.0603541	1265.060312(7)
$\sigma_{LO}^{QED}(m_e = 0)$	1264.9381128	(-)

Table 2: Leading order cross section for MuonE experiment.

Using the above MuonE experiment setup, we can now compare our analytical result with the numerical simulation of [2].

One-loop diagrams



From left to right : Vacuum diagram, Vertex correction diagram, Box diagram. The LSZ reduction formula :

$$i\mathcal{M}_{total} = \prod_{i=1}^4 \sqrt{\tilde{Z}_i} (i\mathcal{M}_{LO} + i\mathcal{M}_{vp} + i\mathcal{M}_{vc} + i\mathcal{M}_{bd}), \quad (5)$$

One-loop integrals

One out of the one-loop integrals we will encounter :

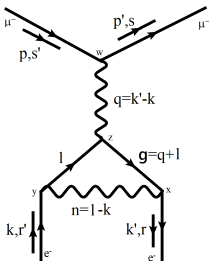


Figure 1: The Vertex correction diagrams

Vertex diagram's amplitude :

$$\begin{aligned}
 i\mathcal{M}_{1,vc} &= \bar{u}_e^r(k')(-e^3) \int \frac{d^4l}{(2\pi)^4} g_{\rho\nu} \frac{\gamma^\nu(\not{g} + m_e)\gamma^\alpha(\not{l} + m_e)\gamma^\rho}{n^2(g^2 - m_e)(l^2 - m_e)} u_e^{r'}(k) \frac{-ig_{\alpha\beta}}{q^2} \cdot \bar{u}_\mu^s(p')(-ie\gamma^\beta)u_\mu^{s'}(p) \\
 &= e^4 \int \frac{d^4l}{(2\pi)^4} \frac{-g_{\rho\nu}g_{\alpha\beta}}{n^2q^2} \bar{u}_e^r(k')\gamma^\nu \frac{i}{\not{g} - m_e} \gamma^\alpha \frac{i}{\not{l} - m_e} \gamma^\rho u_e^{r'}(k) \cdot \bar{u}_\mu^s(p')\gamma^\beta u_\mu^{s'}(p).
 \end{aligned} \tag{6}$$

Dimensional regularization

At one-loop level, we will however meet some interesting problems of one-loop integrals with UV and IR-divergence. With UV-divergence, we are going to use dimensional regularization to parameterize UV divergent values [3] :

$$\frac{16\pi^2}{i} \int \frac{d^4 q}{(2\pi)^4} \dots \rightarrow \frac{(2\pi\mu)^{4-D}}{i\pi^2} \int d^D q \dots = \langle | \dots | \rangle_q, \quad (7)$$

The UV divergence of total amplitude

- The tree-level

$$i\mathcal{M}_0 \sim 1(\alpha).$$

- The Vacuum polarization

$$i\mathcal{M}_{vp} \sim \frac{-2}{3}\Delta(\alpha^2).$$

- The Vertex correction

$$i\mathcal{M}_{vc} \sim \frac{1}{2}\Delta(\alpha^2).$$

- The Box diagrams

$$i\mathcal{M}_{bd} \sim \text{UV-convergent}(\alpha^2).$$

- LSZ factor

$$\tilde{Z}_i \sim 1 - \frac{1}{4}\Delta(\alpha).$$

Total one-loop amplitude :

$$\begin{aligned} i\mathcal{M}_{total} &= \prod_{i=1}^4 \sqrt{\tilde{Z}_i} (i\mathcal{M}_0 + i\mathcal{M}_{vp} + i\mathcal{M}_{vc} + i\mathcal{M}_{bd}) \sim [1 - \frac{1}{2}\Delta(\alpha)] \cdot \left[1(\alpha) - \frac{2}{3}\Delta(\alpha^2) + \frac{1}{2}\Delta(\alpha^2) \right] \\ &\sim \frac{-2}{3}\Delta(\alpha^2) + \frac{1}{2}\Delta(\alpha^2) - \frac{1}{2}\Delta(\alpha^2) \sim \frac{-2}{3}\Delta(\alpha^2). \end{aligned}$$

(8)

Renormalization

To resolve the UV-singularities, we have to use an extra procedure, the Renormalization method, first of all, we must renormalize the QED Lagrangian.

$$\begin{aligned}\mathcal{L}_0 &= \bar{\psi}_0(i\not{\partial} - m_0)\psi_0 - \frac{1}{4}F^{\mu\nu}F_{\mu\nu} - e_0\bar{\psi}_0\not{A}\psi_0 \\ \rightarrow \mathcal{L}_R &= Z_\psi\bar{\psi}(i\not{\partial} - Z_m.m)\psi - \frac{1}{4}Z_AF^{\mu\nu}F_{\mu\nu} - Z_eZ_\psi\sqrt{Z_A}e\bar{\psi}\not{A}\psi,\end{aligned}\tag{9}$$

with :

$$\begin{cases} \psi_0 = \sqrt{Z_\psi}\psi = \sqrt{1 + \delta_\psi}\psi \\ A_0^\mu = \sqrt{Z_A}A^\mu = \sqrt{1 + \delta_A}A^\mu \\ m_0 = Z_m.m = m + \delta_m \\ e_0 = Z_e.e = e + \delta_e \end{cases},\tag{10}$$

where we have expanded perturbatively at one-loop order $Z_i = 1 + \delta_i(\alpha)$.

Renormalization

To resolve the UV-singularities, we have to use an extra procedure, the Renormalization method, first of all, we must renormalize the QED Lagrangian.

$$\begin{aligned}\mathcal{L}_0 &= \bar{\psi}_0(i\not{\partial} - m_0)\psi_0 - \frac{1}{4}F^{\mu\nu}F_{\mu\nu} - e_0\bar{\psi}_0\not{A}\psi_0 \\ \rightarrow \mathcal{L}_R &= Z_\psi\bar{\psi}(i\not{\partial} - Z_m.m)\psi - \frac{1}{4}Z_AF^{\mu\nu}F_{\mu\nu} - Z_eZ_\psi\sqrt{Z_A}e\bar{\psi}\not{A}\psi,\end{aligned}\tag{9}$$

with :

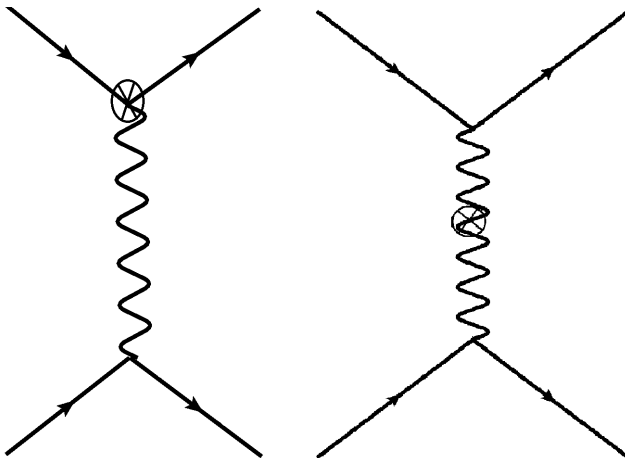
$$\begin{cases} \psi_0 = \sqrt{Z_\psi}\psi = \sqrt{1 + \delta_\psi}\psi \\ A_0^\mu = \sqrt{Z_A}A^\mu = \sqrt{1 + \delta_A}A^\mu \\ m_0 = Z_m.m = m + \delta_m \\ e_0 = Z_e.e = e + \delta_e \end{cases},\tag{10}$$

where we have expanded perturbatively at one-loop order $Z_i = 1 + \delta_i(\alpha)$.

The renormalized Lagrangian reads :

$$\begin{aligned}\mathcal{L}_R &= \bar{\psi}(i\not{\partial} - m)\psi - \frac{1}{4}F^{\mu\nu}F_{\mu\nu} - e\bar{\psi}\not{A}\psi \\ &\quad - \bar{\psi}\delta_m\psi + \delta_\psi\bar{\psi}(i\not{\partial} - m)\psi - \frac{1}{4}\delta_AF_{\mu\nu}F^{\mu\nu} - e\bar{\psi}\not{A}\psi(\delta_e + \delta_\psi + \frac{1}{2}\delta_A) \\ &= \mathcal{L}_R^0 + \mathcal{L}_{\text{counterterm}}.\end{aligned}\tag{11}$$

Counterterm diagram



UV cancellation

- Counterterm amplitude :

$$i\mathcal{M}_{ct} \sim \frac{1}{6} \Delta(\alpha^2). \quad (12)$$

- LSZ factors after Renormalization

$$\begin{aligned} \Rightarrow \tilde{Z}_p &= 1 - \frac{d\hat{\Sigma}^{ff}(\not{p})}{d\not{p}}|_{\not{p}=m} = 1 - \frac{d\Sigma^{ff}(\not{p})}{d\not{p}}|_{\not{p}=m} - \delta_\psi = 1 - \frac{d\Sigma^{ff}(\not{p})}{d\not{p}}|_{\not{p}=m} + 2m \frac{\partial \Sigma^{ff}(p)}{\partial p^2}|_{\not{p}=m} \\ &= 1 - \frac{d\Sigma^{ff}(d\not{p})}{d\not{p}}|_{\not{p}=m} + \frac{\partial \Sigma^{ff}(p)}{\partial p^2} \frac{2\not{p} \partial \not{p}}{\partial \not{p}}|_{\not{p}=m} = 1 - \frac{d\Sigma^{ff}(\not{p})}{d\not{p}}|_{\not{p}=m} + \frac{\partial \Sigma^{ff}(p)}{\partial p^2} \frac{\partial p^2}{\partial \not{p}}|_{\not{p}=m} = 1 \end{aligned} \quad (13)$$

The UV divergence of total amplitude after Renormalization :

Combining the results of renormalized LSZ factors and additional Feynman counterterm amplitude into our previous amplitude Eq.(8) to get UV convergent amplitude after renormalization :

$$\begin{aligned} i\mathcal{M}_{total} &= \prod_{i=1}^4 \sqrt{\tilde{Z}_i} (i\mathcal{M}_0 + i\mathcal{M}_{vp} + i\mathcal{M}_{vc} + i\mathcal{M}_{bd} + i\mathcal{M}_{ct}) \\ &\sim 1. \left[1(\alpha) - \frac{2}{3} \Delta(\alpha^2) + \frac{1}{2} \Delta(\alpha^2) + \frac{1}{6} \Delta(\alpha^2) \right] \sim 0 \Delta \rightarrow \text{UV convergent.} \end{aligned} \quad (14)$$

IR divergence of NLO differential cross section

- The Vacuum polarization

$$i\mathcal{M}_{vp} = 0.i\mathcal{M}_{LO}.$$

- The Vertex correction

$$i\mathcal{M}_{vc} = \frac{e^2}{4\pi^2} \left[-2k'.k \frac{x_{te}}{m_e^2(1-x_{te}^2)} \log(x_{te}) \log\left(\frac{\lambda}{m_e}\right) - 2p'.p \frac{x_{t\mu}}{m_\mu^2(1-x_{t\mu}^2)} \log(x_{t\mu}) \log\left(\frac{\lambda}{m_\mu}\right) \right] .i\mathcal{M}_{LO}.$$

- The Box diagrams

$$i\mathcal{M}_{bd} = \frac{e^2}{4\pi^2} \left[-2k'p' \frac{x_s}{m_e m_\mu (1-x_s^2)} \log(x_s) \log\left(\frac{\lambda^2}{-q^2 - i\epsilon}\right) \right. \\ \left. - 2k'p \frac{x_u}{m_e m_\mu (1-x_u^2)} \log(x_u) \log\left(\frac{\lambda^2}{-q^2 - i\epsilon}\right) \right] .i\mathcal{M}_{LO}.$$

- The counterterm diagrams

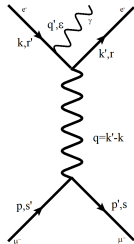
$$i\mathcal{M}_{ct} = \frac{e^2}{4\pi^2} \left[-\log \frac{\lambda}{m_e} - \log \frac{\lambda}{m_\mu} \right] .i\mathcal{M}_{LO}.$$

IR divergence of NLO differential cross section

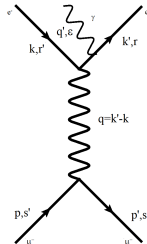
The total virtual differential cross section

$$\begin{aligned} \left(\frac{d\sigma}{d\Omega} \right)_{\text{NLO}}^{\text{Virt}} &= \frac{e^2}{4\pi^2} \left(\frac{d\sigma}{d\Omega} \right)_{\text{LO}} \\ &\times 2\text{Re} \left[-2k' \cdot k \frac{x_{te}}{m_e^2(1-x_{te}^2)} \log(x_{te}) \log\left(\frac{\lambda}{m_e}\right) - 2p' \cdot p \frac{x_{t\mu}}{m_\mu^2(1-x_{t\mu}^2)} \log(x_{t\mu}) \log\left(\frac{\lambda}{m_\mu}\right) - \log \frac{\lambda}{m_e} - \log \frac{\lambda}{m_\mu} \right. \\ &\left. - 2k' p' \frac{x_s}{m_e m_\mu (1-x_s^2)} \log(x_s) \log\left(\frac{\lambda^2}{-q^2 - i\epsilon}\right) - 2k' p \frac{x_u}{m_e m_\mu (1-x_u^2)} \log(x_u) \log\left(\frac{\lambda^2}{-q^2 - i\epsilon}\right) \right] (\alpha^3). \end{aligned} \quad (15)$$

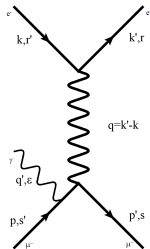
Photon radiation



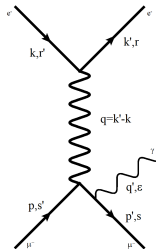
a)



b)



c)



d)

For the calculation at NLO, we have to include the emission of one additional photon. We split this real emission process into two parts as follows :

$$d\sigma_{real}(\alpha^3) = d\sigma_{soft}(\alpha^3) + d\sigma_{hard}(\alpha^3), \quad (16)$$

where the soft-photon region is defined by $E_\gamma \leq \Delta E$ with ΔE being a cutoff parameter. The value of ΔE must be very small compared to the colliding energy.

Soft-photon corrections

Because of the electrons and muons are charged particles, they always emit photons (electromagnetic radiation). The photon emission is therefore an essential part of QED scattering processes. The $e^- \mu^- \rightarrow e^- \mu^-$ scattering without photon emission is actually unphysical and we can't observe this process separately.

In soft-photon emission, we neglect the momentum q' of the radiative photon everywhere except in the denominator of the fermion propagator. We then get the following result for the differential cross section :

$$\left(\frac{d\sigma}{d\Omega}\right)_{\text{Soft}} = - \left(\frac{d\sigma}{d\Omega}\right)_{\text{LO}} \cdot \frac{e^2}{(2\pi)^3} \int_{|q'| \leq \Delta E} \frac{d^3 q'}{2\omega_{q'}} \left[\frac{k^2}{(q'k)^2} + \frac{k'^2}{(q'k')^2} - \frac{2kk'}{q'k \cdot q'k'} + \frac{p^2}{(q'p)^2} + \frac{p'^2}{(q'p')^2} - \frac{2pp'}{q'k \cdot q'k'} \right. \\ \left. + 2\text{Re} \left(\frac{p'k'}{p'q' \cdot k'q'} - \frac{p'k}{p'q' \cdot kq'} - \frac{pk'}{pq' \cdot k'q'} + \frac{pk}{pq' \cdot kq'} \right) \right] (\alpha^3), \quad (17)$$

with $\omega_{q'} = \sqrt{|\vec{q}'|^2 + \lambda^2}$, where λ is the photon mass.

IR divergent part of the *Soft-photon radiation*

The total IR divergent part of the *Soft-photon radiation* differential cross section reads :

$$\begin{aligned} \left(\frac{d\sigma}{d\Omega} \right)_{Soft} &= \frac{-e^2}{4\pi^2} \left(\frac{d\sigma}{d\Omega} \right)_{LO} \cdot \text{Re} \left\{ 4 \log \left(\frac{2\Delta E}{\lambda} \right) + 4kk' \frac{x_{te}}{m_e^2(1-x_t^2)} \log(x_{te}) \log \left(\frac{2\Delta E}{\lambda} \right) \right. \\ &+ 4pp' \frac{x_{t\mu}}{m_\mu^2(1-x_{t\mu}^2)} \log(x_{t\mu}) \log \left(\frac{2\Delta E}{\lambda} \right) + 2 \left[2k'p' \frac{x_s}{m_e m_\mu(1-x_s^2)} \log(x_s) \log \left(\frac{2\Delta E}{\lambda} \right)^2 \right. \\ &\left. \left. + 2k'p \frac{x_u}{m_e m_\mu(1-x_u^2)} \log(x_u) \log \left(\frac{2\Delta E}{\lambda} \right)^2 \right] \right\} (\alpha^3). \end{aligned} \quad (18)$$

We can see that the cross section of soft photon radiation process as IR divergent as the virtual corrections, but with a sign difference.

IR convergent cross section

The IR-divergent part of the NLO cross section reads :

$$\begin{aligned}
 \left(\frac{d\sigma}{d\Omega}\right)_{\text{NLO}}^{\text{IR}} &= \left(\frac{d\sigma}{d\Omega}\right)_{\text{Virt}} + \left(\frac{d\sigma}{d\Omega}\right)_{\text{Soft}} = \frac{-e^2}{4\pi^2} \left(\frac{d\sigma}{d\Omega}\right)_{\text{LO}} \text{Re} \left[\log\left(\frac{2\Delta E}{m_e}\right)^2 + \log\left(\frac{2\Delta E}{m_\mu}\right)^2 \right. \\
 &+ 4kk' \frac{x_{te}}{m_e^2(1-x_{te}^2)} \log(x_{te}) \log\left(\frac{2\Delta E}{m_e}\right) + 4pp' \frac{x_{t\mu}}{m_\mu^2(1-x_{t\mu}^2)} \log(x_{t\mu}) \log\left(\frac{2\Delta E}{m_\mu}\right) \\
 &+ 4k'p' \frac{x_s}{m_em_\mu(1-x_s^2)} \log(x_s) \log\left(\frac{4\Delta E^2}{-q^2-i\epsilon}\right) + 4k'p \frac{x_u}{m_em_\mu(1-x_u^2)} \log(x_u) \log\left(\frac{4\Delta E^2}{-q^2-i\epsilon}\right) \left. \right] (\alpha^3), \\
 &\Rightarrow \left(\frac{d\sigma}{d\Omega}\right)_{\text{NLO}} \text{ is IR convergent .}
 \end{aligned} \tag{19}$$

Next-to-leading order cross section

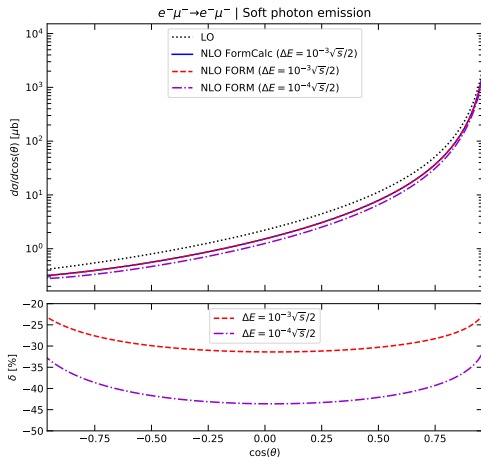
Finally, we define here the NLO cross section :

$$\begin{aligned} d\sigma_{NLO} &= d\sigma_{LO}(\alpha^2) + d\sigma_{virt}(\alpha^3) + d\sigma_{soft}(\alpha^3). \\ &= f(s, t, u, m_e, m_\mu, \Delta E, A_0, B_0, C_0, D_0, \dots) \end{aligned} \quad (20)$$

The output of my FORM program calculating squared one-loop amplitude depends on the kinematical variables s, t, u and the one-loop functions $A_0, B_0, C_0, D_0, B_1, C_1, \dots$. To cross check the squared amplitude output of my FORM program, we have used the FormCalc-6.2 [4] and FeynArts-3.4 [5] to generate another expression for the squared amplitude. The scalar and tensor loop integrals for both FormCalc and FORM results are calculated by the LoopInts library³. The input parameters are the same as the MUonE experiment.

³I thank Le Duc Ninh for providing the FormCalc results and for performing the numerical calculation for results of FORM

Next-to-leading order numerical results



In Fig. (2), the δ is defined as:

$$\delta = \frac{d\sigma_{NLO} - d\sigma_{LO}}{d\sigma_{LO}}. \quad (21)$$

Take a look in the two figures, the FORM results are identical to FormCalc. The relative correction δ can change dramatically as the cutoff ΔE be smaller because of $\log(\Delta E)$ dependence in $d\sigma_{Soft}$.

Figure 2: LO and NLO differential cross section in $\cos \theta$

Conclusion

From the work of this thesis, we can draw the following conclusions :

- The t-channel divergence occurring in the LO total cross section is due to the infinite range of the electromagnetic interaction.
- We have successfully cancelled out all divergences occurring at next-to-leading order, UV divergence is cancelled by renormalization and IR divergence by adding soft-photon corrections. We note that the photon radiation is an indispensable part of the scattering process of charged particles.
- Our final NLO amplitudes are identical to results of FormCalc program.

Outlook

- Include the missing hard photon corrections.
- Include the electroweak corrections in the Standard Model.
- Write a Mathematica code to calculate all the one-loop integrals of the $e^- \mu^- \rightarrow e^- \mu^-$ process.

References



G. Abbiendi et al.

Measuring the leading hadronic contribution to the muon $g-2$ via μe scattering.
Eur. Phys. J. C, 77(3):139, 2017.



Massimo Alacevich, Carlo M. Carloni Calame, Mauro Chiesa, Guido Montagna, Oreste Nicrosini, and Fulvio Piccinini.
Muon-electron scattering at NLO.
JHEP, 02:155, 2019.



Matthias Steinhauser.

Übungen zu strahlungskorrekturen in eichtheorien.
II. Institut für Theoretische Physik, Universität Hamburg, 22761 Hamburg, 2003.



T. Hahn and M. Perez-Victoria.

Automatized one loop calculations in four-dimensions and D-dimensions.
Comput. Phys. Commun., 118:153–165, 1999.



Thomas Hahn.

Generating Feynman diagrams and amplitudes with FeynArts 3.
Comput. Phys. Commun., 140:418–431, 2001.



A. Denner and S. Dittmaier.

Scalar one-loop 4-point integrals.
Nucl. Phys. B, 844:199–242, 2011.

THANKS FOR YOUR
ATTENTION

Renormalization conditions

These conditions require that those renormalized functions have a tree-level form in the on-shell limit ($p^2 = m^2$). This is the on-shell renormalization scheme :

- Condition 1 - Dirac equation :

$$\tilde{R}\hat{e}\hat{f}^f(p)u(p)|_{p^2=m^2} = 0$$

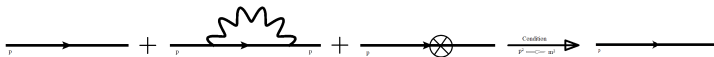
$$\Rightarrow \delta_m = \tilde{R}e\Sigma^f(m) = \frac{e^2}{8\pi^2} \left[mB_1(m^2, 0, m) - mB_0(m^2, 0, m) + \frac{m}{2} \right].$$

slide

Renormalization conditions

These conditions require that those renormalized functions have a tree-level form in the on-shell limit ($p^2 = m^2$). This is the on-shell renormalization scheme :

- Condition 2 :



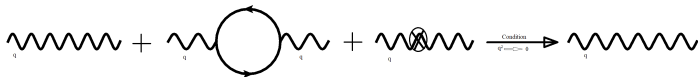
$$\lim_{p^2 \rightarrow m^2} \frac{\not{p} + m}{p^2 - m^2} \tilde{R}e\hat{\Gamma}^{ff}(p)u(p) = iu(p)$$

$$\begin{aligned} \Rightarrow \delta_{\psi_j} &= -2m_j \tilde{R}e \frac{\partial \Sigma^{ff}(p)}{\partial p^2} \Big|_{\not{p}=m_j} = -2m_j \frac{\partial \Sigma^{ff}(p)}{\partial p^2} \Big|_{\not{p}=m_j} \\ &= \frac{m_j e^2}{4\pi^2} \left[-\frac{B_1(m_j^2, 0, m_j)}{2m_j} - \frac{B_0(m_j^2, 0, m_j)}{2m_j} - m_j \frac{\partial B_1(p^2, 0, m_j)}{\partial p^2} \Big|_{p^2=m_j^2} \right. \\ &\quad \left. + m_j \frac{\partial B_0(p^2, 0, m_j)}{\partial p^2} \Big|_{p^2=m_j^2} + \frac{1}{4m_j} \right]. \end{aligned}$$

Renormalization conditions

These conditions require that those renormalized functions have a tree-level form in the on-shell limit ($p^2 = m^2$). This is the on-shell renormalization scheme :

- Condition 3:



$$\lim_{q^2 \rightarrow 0} \frac{1}{q^2} \text{Re} \hat{\Gamma}_{\mu\nu}^{AA}(q) \epsilon^\nu(q) = -i \epsilon_\mu(q)$$

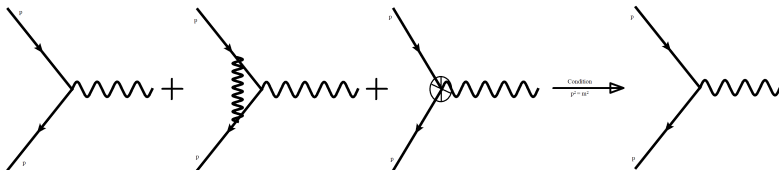
$$\Rightarrow \delta_A = \frac{-e^2}{4\pi^2} \sum_{j=e,\mu} \text{Re} \left[-\frac{1}{9} + \frac{2}{3} m_j^2 B'_0(q^2, m_j, m_j) \Big|_{q^2=0} + \frac{B_1(0, m_j, m_j)}{3} + \frac{B_0(0, m_j, m_j)}{2} \right].$$

slide

Renormalization conditions

These conditions require that those renormalized functions have a tree-level form in the on-shell limit ($p^2 = m^2$). This is the on-shell renormalization scheme :

• Condition 4 :



$$\bar{u}(p) \hat{\Gamma}_{\mu}^{Aff}(p, p) u(p) \Big|_{p^2=m^2} = -ie \bar{u}(p) \gamma_{\mu} u(p)$$

$$\Rightarrow \delta_e = -\frac{1}{2} \delta_A.$$

slide

Notations

$$A_0(m) = \langle | \left(q^2 - m^2 + i\epsilon \right)^{-1} | \rangle_q \quad (22)$$

$$B_0(p, m_0, m_1) = \langle | \left[(q^2 - m_0^2 + i\epsilon) \left((q+p)^2 - m_1^2 + i\epsilon \right) \right]^{-1} | \rangle_q \quad (23)$$

$$B_\mu(p, m_0, m_1) = \langle | q_\mu \left[(q^2 - m_0^2 + i\epsilon) \left((q+p)^2 - m_1^2 + i\epsilon \right) \right]^{-1} | \rangle_q \quad (24)$$

$$B_{\mu\nu}(p, m_0, m_1) = \langle | q_\mu q_\nu \left[(q^2 - m_0^2 + i\epsilon) \left((q+p)^2 - m_1^2 + i\epsilon \right) \right]^{-1} | \rangle_q \quad (25)$$

$$C_0(p, p', m_0, m_1, m_2) = \langle | \left[(q^2 - m_0^2 + i\epsilon) \left((q+p)^2 - m_1^2 + i\epsilon \right) \left((q+p')^2 - m_2^2 + i\epsilon \right) \right]^{-1} | \rangle_q \quad (26)$$

$$C_\mu(p, p', m_0, m_1, m_2) = \langle | q_\mu \left[(q^2 - m_0^2 + i\epsilon) \left((q+p)^2 - m_1^2 + i\epsilon \right) \left((q+p')^2 - m_2^2 + i\epsilon \right) \right]^{-1} | \rangle_q \quad (27)$$

$$C_{\mu\nu}(p, p', m_0, m_1, m_2) = \langle | q_\mu q_\nu \left[(q^2 - m_0^2 + i\epsilon) \left((q+p)^2 - m_1^2 + i\epsilon \right) \left((q+p')^2 - m_2^2 + i\epsilon \right) \right]^{-1} | \rangle_q \quad (28)$$

$$D_0(p, p_1, p_2, m_0, m_1, m_2, m_3) = \langle | \left[(q^2 - m_0^2 + i\epsilon) \left((q+p)^2 - m_1^2 + i\epsilon \right) \left((q+p_1)^2 - m_2^2 + i\epsilon \right) \right. \right. \\ \left. \left. \left((q+p_2)^2 - m_3^2 + i\epsilon \right) \right]^{-1} | \rangle_q \quad (29)$$

$$D_\mu(p, p_1, p_2, m_0, m_1, m_2, m_3) = \langle | q_\mu \left[(q^2 - m_0^2 + i\epsilon) \left((q+p)^2 - m_1^2 + i\epsilon \right) \left((q+p_1)^2 - m_2^2 + i\epsilon \right) \right. \right. \\ \left. \left. \left((q+p_2)^2 - m_3^2 + i\epsilon \right) \right]^{-1} | \rangle_q \quad (30)$$

$$D_{\mu\nu}(p, p_1, p_2, m_0, m_1, m_2, m_3) = \langle | q_\mu q_\nu \left[(q^2 - m_0^2 + i\epsilon) \left((q+p)^2 - m_1^2 + i\epsilon \right) \left((q+p_1)^2 - m_2^2 + i\epsilon \right) \right. \right. \\ \left. \left. \left((q+p_2)^2 - m_3^2 + i\epsilon \right) \right]^{-1} | \rangle_q \quad (31)$$

Vacuum polarization amplitudes

Vacuum polarization

$$i\mathcal{M}_{1,vp} = \frac{-ie^4}{q^4 4\pi^2} \bar{u}_e^r(k') \gamma^\mu u_e^{r'}(k) \bar{u}_\mu^s(p') \gamma^\nu u_\mu^{s'}(p) \left\{ 2B_{\mu\nu}(q, m_e, m_e) + q_\mu B_\nu(q, m_e, m_e) + q_\nu B_\mu(q, m_e, m_e) \right. \\ \left. + \left[\frac{q^2}{2} B_0(q^2, m_e, m_e) - A_0(m_e) \right] g_{\mu\nu} \right\}, \quad (32)$$

and :

$$i\mathcal{M}_{2,vp} = \frac{-ie^4}{q^4 4\pi^2} \bar{u}_e^r(k') \gamma^\mu u_e^{r'}(k) \bar{u}_\mu^s(p') \gamma^\nu u_\mu^{s'}(p) \left\{ 2B_{\mu\nu}(q, m_\mu, m_\mu) + q_\mu B_\nu(q, m_\mu, m_\mu) + q_\nu B_\mu(q, m_\mu, m_\mu) \right. \\ \left. + \left[\frac{q^2}{2} B_0(q^2, m_\mu, m_\mu) - A_0(m_\mu) \right] g_{\mu\nu} \right\}. \quad (33)$$

Vertex correction amplitudes

Vertex correction

$$\begin{aligned} i\mathcal{M}_{1,vc} = & \frac{ie^4}{q^2 16\pi^2} \bar{u}_e^r(k') \left\{ -2\gamma^\alpha - 2\gamma^\mu \gamma^\alpha \gamma^\nu \left[C_{\mu\nu}(k, k', 0, m_e, m_e) + k_\mu C_\nu(k, k', 0, m_e, m_e) + k_\nu C_\mu(k, k', 0, m_e, m_e) \right. \right. \\ & + k_\mu k_\nu C_0(k, k', 0, m_e, m_e) + q_\nu C_\mu(k, k', 0, m_e, m_e) + q_\nu k_\mu C_0(k, k', 0, m_e, m_e) \left. \right] + 8m_e \left[C^\alpha(k, k', 0, m_e, m_e) \right. \\ & \left. \left. + k^\alpha C_0(k, k', 0, m_e, m_e) \right] + 4m_e q^\alpha C_0(k, k', 0, m_e, m_e) - 2m_e^2 \gamma^\alpha C_0(k, k', 0, m_e, m_e) \right\} u_e^{r'}(k) \bar{u}_\mu^s(p') \gamma_\alpha u_\mu^{s'}(p), \end{aligned} \quad (34)$$

and :

$$\begin{aligned} i\mathcal{M}_{2,vc} = & \frac{ie^4}{q^2 16\pi^2} \bar{u}_e^r(k') \gamma_\alpha u_\mu^{r'}(k) \bar{u}_\mu^s(p') \left\{ -2\gamma^\alpha - 2\gamma^\mu \gamma^\alpha \gamma^\nu \left[C_{\mu\nu}(p, p', 0, m_\mu, m_\mu) + p_\mu C_\nu(p, p', 0, m_\mu, m_\mu) \right. \right. \\ & + p_\nu C_\mu(p, p', 0, m_\mu, m_\mu) + p_\mu p_\nu C_0(p, p', 0, m_\mu, m_\mu) - q_\nu C_\mu(p, p', 0, m_\mu, m_\mu) - q_\nu p_\mu C_0(p, p', 0, m_\mu, m_\mu) \left. \right] \\ & - 4m_\mu q^\alpha C_0(p, p', 0, m_\mu, m_\mu) + 8m_\mu \left[C^\alpha(p, p', 0, m_\mu, m_\mu) + p^\alpha C_0(p, p', 0, m_\mu, m_\mu) \right] \\ & \left. - 2m_\mu^2 \gamma^\alpha C_0(p, p', 0, m_\mu, m_\mu) \right\} u_\mu^{s'}(p). \end{aligned} \quad (35)$$

Box diagrams

$$\begin{aligned}
 i\mathcal{M}_{1,bd} = \frac{ie^4}{16\pi^2} & \left[4\bar{u}_e^r(k')\gamma^\nu u_e^{r'}(k)\bar{u}_\mu^s(p')\gamma_\nu u_\mu^{s'}(p)k'p'D_0(-q, -k', p', 0, 0, m_e, m_\mu) \right. \\
 & + \bar{u}_e^r(k')\gamma^\nu u_e^{r'}(k)\bar{u}_\mu^s(p')2\not{k}'\gamma^\alpha\gamma_\nu u_\mu^{s'}(p)D_\alpha(-q, -k', p', 0, 0, m_e, m_\mu) \\
 & - \bar{u}_e^r(k')2\not{p}'\gamma^\alpha\gamma^\nu u_e^{r'}(k)\bar{u}_\mu^s(p')\gamma_\nu u_\mu^{s'}(p)D_\alpha(-q, -k', p', 0, 0, m_e, m_\mu) \\
 & \left. - \bar{u}_e^r(k')\gamma^\mu\gamma^\alpha\gamma^\nu u_e^{r'}(k)\bar{u}_\mu^s(p')\gamma_\mu\gamma^\beta\gamma_\nu u_\mu^{s'}(p)D_{\alpha\beta}(-q, -k', p', 0, 0, m_e, m_\mu) \right], \tag{36}
 \end{aligned}$$

and :

$$\begin{aligned}
 i\mathcal{M}_{2,bd} = \frac{ie^4}{16\pi^2} & \left[4\bar{u}_e^r(k')\gamma^\nu u_e^{r'}(k)\bar{u}_\mu^s(p')\gamma_\nu u_\mu^{s'}(p)k'pD_0(-q, -k', -p, 0, 0, m_e, m_\mu) \right. \\
 & - \bar{u}_e^r(k')\gamma^\nu u_e^{r'}(k)\bar{u}_\mu^s(p')\gamma^\nu\gamma_\alpha 2\not{k}'u_\mu^{s'}(p)D_\alpha(-q, -k', -p, 0, 0, m_e, m_\mu) \\
 & - \bar{u}_e^r(k')2\not{p}\gamma^\alpha\gamma^\nu u_e^{r'}(k)\bar{u}_\mu^s(p')\gamma_\nu u_\mu^{s'}(p)D_\alpha(-q, -k', -p, 0, 0, m_e, m_\mu) \\
 & \left. + \bar{u}_e^r(k')\gamma^\mu\gamma^\alpha\gamma^\nu u_e^{r'}(k)\bar{u}_\mu^s(p')\gamma_\nu\gamma^\beta\gamma_\mu u_\mu^{s'}(p)D_{\alpha\beta}(-q, -k', -p, 0, 0, m_e, m_\mu) \right]. \tag{37}
 \end{aligned}$$

LSZ factors

$$\tilde{Z}_p = 1 + \frac{e^2}{16\pi^2} \{ [-2B_0(m_\mu, 0, m_\mu) - 2B_1(m_\mu, 0, m_\mu) + 1] + \not{p} \frac{d\Sigma_V(p)}{d\not{p}} + 2m_\mu \frac{d\Sigma_S(p)}{d\not{p}} \} |_{\not{p}=m_\mu}. \quad (38)$$

$$\tilde{Z}_{p'} = 1 + \frac{e^2}{16\pi^2} \{ [-2B_0(m_\mu, 0, m_\mu) - 2B_1(m_\mu, 0, m_\mu) + 1] + \not{p}' \frac{d\Sigma_V(p')}{d\not{p}'} + 2m_\mu \frac{d\Sigma_S(p')}{d\not{p}'} \} |_{\not{p}'=m_\mu}. \quad (39)$$

$$\tilde{Z}_{k'} = 1 + \frac{e^2}{16\pi^2} \{ [-2B_0(m_e, 0, m_e) - 2B_1(m_e, 0, m_e) + 1] + \not{k}' \frac{d\Sigma_V(k')}{d\not{k}'} + 2m_e \frac{d\Sigma_S(k')}{d\not{k}'} \} |_{\not{k}'=m_e}. \quad (40)$$

$$\tilde{Z}_k = 1 + \frac{e^2}{16\pi^2} \{ [-2B_0(m_e, 0, m_e) - 2B_1(m_e, 0, m_e) + 1] + \not{k} \frac{d\Sigma_V(k)}{d\not{k}} + 2m_e \frac{d\Sigma_S(k)}{d\not{k}} \} |_{\not{k}=m_e}. \quad (41)$$

UV divergent parts

UV divergent parts of N-point functions : (Represent UV divergent term by Δ)

- $A_0(m) = m^2 \Delta$,
- $B_0(p^2, m_0, m_1) = \Delta$,
- $B_\mu(p, m_0, m_1) = \frac{-1}{2} p_\mu \Delta$,
- $B_1 (B_\mu = p_\mu \cdot B_1) = \frac{-1}{2} \Delta$,
- $B_{\mu\nu}(p, m_0, m_1) = \frac{-g_{\mu\nu}}{12} [p^2 - 3(m_0^2 + m_1^2)] \Delta + \frac{p_\mu p_\nu}{3} \Delta$,
- $C_{\mu\nu}(p, p', m_0, m_1, m_2) = g_{\mu\nu} C_{00}(p, p', m_0, m_1, m_2) = \frac{g_{\mu\nu}}{4} \Delta$,

where $\Delta = \frac{2}{4-D} - \gamma_E + 1$, D is the dimensions of the loop integrals and γ_E is the Euler constant.

Counterterm diagrams

$$i\mathcal{M}_{ct} = \frac{ie^2}{q^2} \bar{u}_e^r(k') \gamma_\alpha u_\mu^{r'}(k) \bar{u}_\mu^s(p') \gamma^\alpha u_\mu^{s'}(p) \left(2\delta_e + \delta_{\psi_e} + \delta_{\psi_\mu} \right), \quad (42)$$

with the counterterm factors are determined by renormalization conditions:

$$\delta_e = \frac{e^2}{8\pi^2} \sum_{j=e,\mu} \text{Re} \left[-\frac{1}{9} + \frac{2}{3} m_j^2 \frac{\partial}{\partial q^2} B_0(q^2, m_j, m_j) \right]_{q^2=0} + \frac{B_1(0, m_j, m_j)}{3} + \frac{B_0(0, m_j, m_j)}{2}, \quad (43)$$

$$\delta_{\psi_j} = \frac{m_j e^2}{4\pi^2} \left[-\frac{B_1(m_j^2, 0, m_j)}{2m_j} - \frac{B_0(m_j^2, 0, m_j)}{2m_j} - m_j \frac{\partial B_1(p^2, 0, m_j)}{\partial p^2} \right]_{p^2=m_j^2} + m_j \frac{\partial B_0(p^2, 0, m_j)}{\partial p^2} \Big|_{p^2=m_j^2} + \frac{1}{4m_j}, \quad (44)$$

$$\delta_A = \frac{-e^2}{4\pi^2} \sum_{j=e,\mu} \text{Re} \left[-\frac{1}{9} + \frac{2}{3} m_j^2 B_0'(q^2, m_j, m_j) \right]_{q^2=0} + \frac{B_1(0, m_j, m_j)}{3} + \frac{B_0(0, m_j, m_j)}{2}. \quad (45)$$

